

High-efficiency ^{99}Tc separation from contaminated liquid waste using some anion exchange resins

Debasish Das*

Waste Management Division, Bhabha Atomic Research Centre, Trombay, Mumbai-400085, India

*Corresponding author: deba.chem@gmail.com, debads@barc.gov.in

ABSTRACT

^{99}Tc removal from contaminated aqueous solution was explored using some commercially available anion exchange resins with various specifications. Various combinations of physicochemical parameters like polymeric network, pore diameter, percent cross-linking, bead size etc. were selected to appraise their impact on ^{99}Tc uptake. Fundamental extraction properties such as effect of solution pH, equilibration time, effect of temperature were determined for obtaining the optimum extraction condition. The resins were characterized using BET, SEM, EDS, XPS, TG, FTIR spectroscopy to decipher the structure-extraction correlation and extraction mechanism. In order to quantify the loading capacity (745 mg/g as maximum) and ascertain the reaction mechanism, non-radioactive surrogate of TcO_4^- , i.e, ReO_4^- have been used. ReO_4^- quantity in solution was measured using UV-Vis spectrophotometry with λ_{max} at 204 nm. 4M HNO_3 was found to be an effective reagent towards desorption from the loaded resins. The capture performance was found to deteriorate with γ -radiation particularly at higher absorbed dose (500 kGy onwards). Competition studies with most common anions found in ground water as well as soil such as Cl^- , NO_3^- , SO_4^{2-} , CO_3^{2-} , PO_4^{3-} indicate that, even in presence of high concentration (1:10000 molar ratio) of these interfering anions, TcO_4^- can be selectively extracted by the resins confirming their effectiveness towards the decontamination of real ground water with respect to ^{99}Tc .

Keywords: Wastewater treatment, Sorption, Ion-exchange, ^{99}Tc separation, Desalination, Organic resins.

1. INTRODUCTION

In order to support the increasing global energy demand, power production from nuclear reaction took a pioneer path over other conventional energy production routes.¹⁻⁴ Nuclear fission inside a reactor produces many radioactive fission products along with minor actinides and activation

products. ^{99}Tc is one of the fission products generated during nuclear fission and one important radionuclide towards the environmental and nuclear waste management concern due to its high mobility (water solubility of TcO_4^- is 11.3 mol L^{-1} at 20°C), high fission yield (6.05% for thermal reactor ^{235}U fission) and long half-life ($t_{1/2} = 2.13 \times 10^5$ years).⁵⁻⁷ Moreover, $^{99\text{m}}\text{Tc}$ ($t_{1/2} = 6.04$ hours) is extensively used for medical diagnosis and nuclear medicine for cancer treatment globally. The used radiopharmaceutical should be properly managed before their disposal. Technetium is present in the environment only in the form of radioactive ^{99}Tc with its most stable chemical formula TcO_4^- , i.e., pertechnetate.⁸ Pertechnetate is an anionic species where the oxidation state of Tc is +7 like many other anionic species like MnO_4^- , OsO_4^- , CrO_4^- , ReO_4^- etc. Therefore, TcO_4^- is highly mobile in aquatic and soil environment, and poses a serious problem related to the groundwater contamination.^{9,10}

Many types of materials such as layered double hydroxides (LDH) as pure inorganic materials, molecular complexes, metal-organics frameworks (MOF), covalent organic frameworks (COF), ion-exchange resins, have shown their potential for capturing TcO_4^- from aqueous solution.¹¹⁻²¹ Layered double hydroxides are formed by positively charged layers with charge balancing anion disposed at the interlayer position which is replaceable by TcO_4^- present in aqueous solution. Mg-Al LDH and Ni-Al LDH are found to be the most promising candidates among these.¹⁴ Molecular and supramolecular complexes (e.g., calixarenes and cryptands) have been exploited for the TcO_4^- removal from aqueous solution.⁹ MOFs and COFs have been increasingly become popular day by day because of possibility of carrying ionic frameworks (i-MOFs and i-COFs) due to the presence of ionic side chains, extra-framework ions or simply stoichiometric imbalance between metal centers and organic linkers in case of MOFs. Many similar MOFs and COFs have shown high ability to remove ^{99}Tc from aqueous waste solutions.^{16-18,21} Among all type of materials tested for separating TcO_4^- , polymeric organic anion-exchange resins have shown to be the most promising results.²²⁻²⁷ This is due to the ease of synthesis, large availability, easy of functionalization, regeneration feasibility, high throughput etc. These are mostly styrene and divinyl benzene or polyacrylic backbone based organic polymers functionalized according to the target element to be separated. Polymeric backbone is anionic functionalized in nature if the target element present in the solution as cation and vice versa. The counter ions present in the resin materials are electrostatically attached with the organic polymer, which can be replaced by the ions present in the aqueous medium with different affinity. The

affinity of targeted cation or anion can be increased by modulating different properties of any resin such as functional groups, surface area, percentage cross-linking, counter ions present etc. Many mono and bifunctional resins have been synthesized and developed for selective TcO_4^- removal till today.^{23,26,28-30} Whereas the monofunctional resins were found to be very selective in many cases, these resins have shown poor kinetics. To overcome this problem many bifunctional resins have been developed for real life applications where both selectivity as well as kinetics have been improved.^{28,30} Although many such resins are reported towards their application for TcO_4^- uptake, there is still scope for improvement in terms of selectivity and kinetics. Improved selectivity can help to load the resin with $^{99}\text{TcO}_4^-$ while keeping minimum uptake with respect to other interfering anions. On the other hand, improved kinetics assists to load the resin very fast so that column operation can be more feasible. Nevertheless, to improve the selectivity and kinetic factor, it is very important to understand the role of the structure, physical and other chemical properties of the resins in details.

Herein, we report the uptake properties of TcO_4^- by some commercial anion exchange resins with various chemical and physical properties. While some of the resins are strong base anion exchange type, others are weak base resins. Few resins have gel type morphology with non-porous surface, others are macroreticular type of resins. The macroreticular resins have been selected for the present study with varying pore size. The percentage cross-linking of the resins are also different for different materials. Finally, while selecting the resins, the variation of bead diameter has also been taken into account. The structure-uptake correlation and reaction mechanism is explored in details. Different operational parameters like pH effect, kinetics, thermodynamics, desorption, radiation effect, competition with common anions were determined for their practical applications.

2. EXPERIMENTAL

2.1. Reagents and chemicals

All the reagents used for the present study were of analytical grade. The reagents were used without further purification unless mentioned otherwise. Solution pH was adjusted using dilute HNO_3 or NaOH solution whenever required. All the resins were supplied by Ion Exchange Corporation of India Ltd, Mumbai. The physical and chemical properties of the resins are tabulated in table 1.

Table 1. Resins selected in the present study with their physicochemical properties

Resin name	Type	Functional group	Structure	Density (g/cc)	Matrix	Ionic form as supplied	Total exchange capacity (meq/ml)	Moisture content	Particle size range (nm)
GS300	Strong base type-1	Quaternary ammonium benzyl trimethyl amine	Gel type	0.626	Styrene divinylbenzene copolymer	Chloride	1.3 (minimum)	48-58 %	0.3-1.2
810	Strong base type-1	Quaternary ammonium benzyl trimethyl amine	Macroporous	0.627	Styrene divinylbenzene copolymer	Chloride	1.0 (minimum)	56-63 %	0.3-1.2
820	Strong base type-2	Quaternary ammonium benzyl dimethyl ethanolamine	Macroporous	0.558	Styrene divinylbenzene copolymer	Chloride	1.0 (minimum)	54-61 %	0.3-1.2
830	Strong base type-1	Quaternary ammonium	Macroporous	0.592	Styrene divinylbenzene copolymer	Chloride	0.95 (minimum)	57-66 %	0.3-1.2
890	Weak base	Tertiary amine	Macroporous	0.565	Styrene divinylbenzene copolymer	Free base	1.4 (minimum)	52-56 %	0.3-1.2
930	Strong base type-1	Quaternary ammonium	Macroporous	0.596	polyacrylic divinylbenzene copolymer	Chloride	0.8 (minimum)	65-72 %	0.3-1.2

It can be noted from the table that, the resins were chosen with variation in the chemical type (strong base type-1, strong base type-2, weak base), functional groups (quaternary (alkyl, alkanol) amine, tertiary amine), structure (gel or macroporous), base matrix of polymer (styrene or acrylic), ionic form (chloride or free base), exchange capacity (0.8-1.4 meq/ml), moisture content etc.

^{99m}Tc was supplied by Board of Radiation and Isotope Technology (BRIT), Mumbai, India. It was obtained after subsequent decay of $^{99\text{m}}\text{Tc}$ (a well-known radiopharmaceutical source), which is separated after milking of $^{99\text{m}}\text{Tc}$ from $^{99}\text{Mo}/^{99\text{m}}\text{Tc}$ generator. Pure $^{99\text{m}}\text{Tc}$ is obtained after loading ^{99}Mo containing solution onto an acidic alumina column followed by selective elution of $^{99\text{m}}\text{Tc}$ in the form of $^{99\text{m}}\text{TcO}_4^-$ by passing a 0.9M NaCl solution through the column. The supplied $^{99\text{m}}\text{Tc}$ was in the form of high purity $\text{Na}^{99\text{m}}\text{TcO}_4$ solution with slight contamination of ^{99}Mo and non-radioactive Al.

2.2. Measurement and techniques

The experiments were conducted using $^{99\text{m}}\text{Tc}$ tracer solution. Radioactivity of the solutions before and after equilibration was measured using a liquid scintillation counter (model: Triathler,

Hidex). 50 μL sample was added into 2 mL scintillation cocktail (Cocktail W, SRL India), waited for 15 minutes, and counted for 300 sec for all the measurements. Calibration curves with different quench parameters (Q_P) values were plotted (% efficiency vs Q_P) for the ^{99}Tc standard solution to establish the chemical and colour quenching effect (HNO_3 and nitromethane were used as chemical and colour quencher respectively). These curves were used to find out the exact specific activity of the solutions under study. For non-radioactive set of studies, chemical surrogate of TcO_4^- , ReO_4^- was used in the form of NH_4ReO_4 . Concentration of ReO_4^- was measured by using UV-Vis spectrophotometry with λ_{max} at 203 and 227 nm. Pore size and surface area of the resins was measured by putting the samples in BET analyzer. The samples were preheated at 100°C before starting the actual N_2 absorption step. Thermal stability of the resins was analyzed using thermogravimetric technique. Particle size and morphology of the resin samples were determined using scanning electron microscope (SEM). ReO_4^- distribution on the resin beads was investigated by elemental mapping using energy dispersive X-ray spectroscopy (EDS). Elemental constituents and chemical form of the resin beads before and after equilibrating with ReO_4^- were assessed by recording X-ray photoelectron spectroscopy (XPS). To ascertain the reaction mechanism, the beads were analyzed by Fourier Transform infrared spectroscopy (FTIR) spectroscopy before and after equilibrating with ReO_4^- . Concentration of Cl^- , NO_3^- , SO_4^{2-} , CO_3^{2-} , and PO_4^{3-} were monitored using ion-chromatography (Dionex-DX-500, consisting of a self-regenerator suppressor ASRS-II and a conductivity detector-ED-40).

2.3. Batch extraction studies

In order to optimize the extraction condition, batch extraction experiments were conducted with varying solution pH, contact time, initial concentration etc. pH of $^{99}\text{TcO}_4^-$ bearing feed solution was systematically varied from pH = 1 to pH = 11 and used for the extraction studies. The corresponding distribution coefficient K_d (mL/g) is calculated from the following equation:

$$K_d = \frac{(\text{Initial feed activity} - \text{final activity in raffinate})}{\text{final activity in raffinate}} \times \frac{\text{volume of solution equilibrated}}{\text{weight of resin}} \dots (1)$$

K_d^{Eq} (mL/mequiv) is also calculated for determining relative affinity of the resins towards TcO_4^- per ion-exchange site. This is calculated by dividing K_d (mL/g) by total anion exchange capacity, TAEC (mequiv/g) of the particular resin. This signifies the selectivity of the resins with respect to TcO_4^- anion. Equilibration time was varied up to 132 hours to find out the optimized contact

time for solid-liquid two phase extraction. Desorption experiments were conducted by equilibrating loaded beads with different reagents such as NaCl, HNO₃, HCl, NaNO₃ at 4M concentration. To monitor the extraction competition between pertechnetate and most common anions present in the environment, bianionic solutions with pertechnetate as common anion were equilibrated at pH = 7 and the concentration of the ions were analyzed either using ion-chromatographic method. To check the effect of radiation on the resins towards ⁹⁹Tc separation, the resin samples were irradiated at different γ -dose (250 kGy, 500 kGy, and 1000 kGy) inside a gamma chamber equipped with ⁶⁰Co source. These irradiated resins were used for further equilibrium with ⁹⁹Tc feed solution at optimum condition to check their ⁹⁹Tc removal efficacy.

3. RESULTS AND DISCUSSION

3.1. Effect of solution pH

In order to find out the optimum solution pH, pH of the ⁹⁹Tc bearing aqueous solution was systematically varied from 1 to 11 with a step of one unit (1, 3, 5, 7, 9, 11) and equilibrated with all the selected resins separately. For this purpose, 5 mg of each resin was equilibrated with 1 mL ⁹⁹Tc containing solution for 1 hour. The mixture in a 10 mL capacity plastic centrifuge tube was rotated using a tube rotator at 50 rpm. The extraction pattern is represented in Fig. 1. It can be observed that, the amount of ⁹⁹Tc extraction from the aqueous solution to the solid phase has attained a plateau after pH = 3 for some of the resins. For other resins, maximum K_d is observed at pH = 7 which get decreased both the sides. These observations can be explained on the basis of NO₃⁻ and OH⁻ ion competition at lower and higher pH (adjusted with dilute HNO₃ and NaOH) respectively. Similar observation was observed in case of Reillex-HPQ and Dowex 1X8 resins towards TcO₄⁻ uptake.^{23,24} Moreover at higher pH (> 7), there is a chance of losing ion-exchange property particularly for weak base anion exchange resins. As we are more concerned regarding the ⁹⁹Tc separation from low level radioactive waste and environmental effluent, where pH remains invariable at around 7, the results obtained from the pH experiments are very interesting and advantageous for further studies. Therefore, additional experiments were conducted with ⁹⁹Tc containing aqueous solutions at pH = 7.

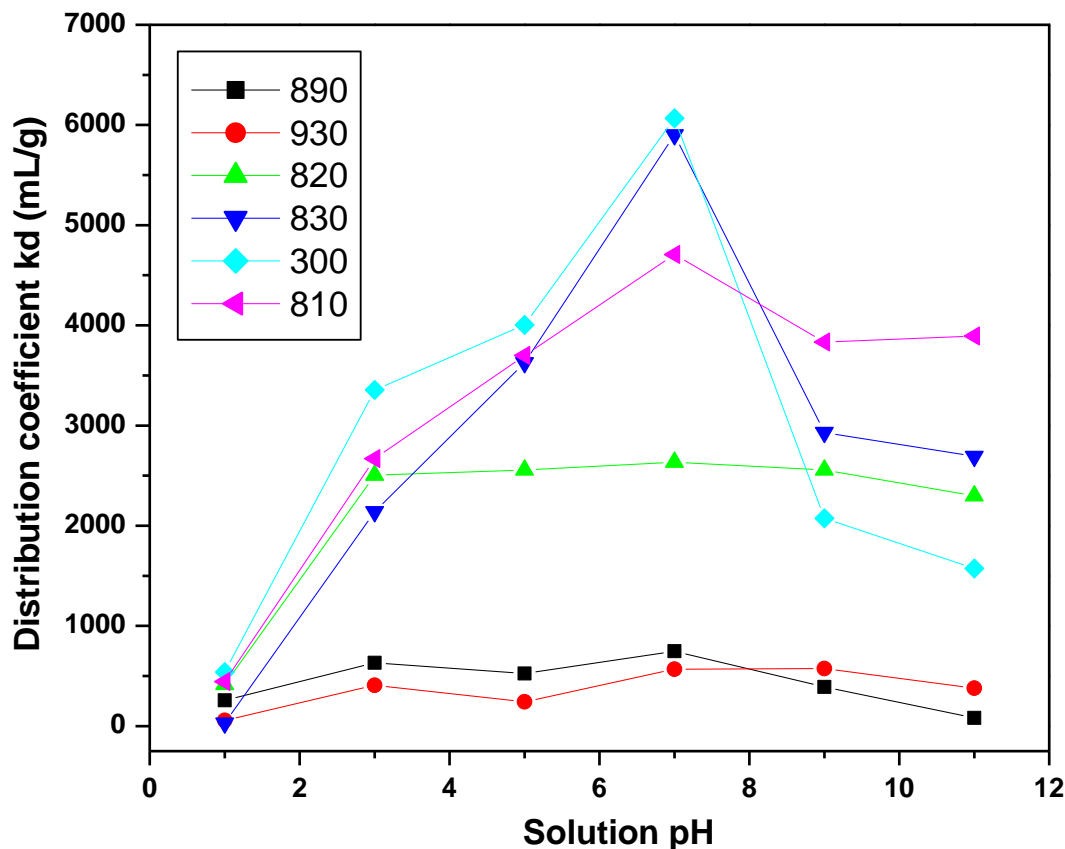


Figure 1. Effect of solution pH; equilibration time: 1 h, rotation: 50 rpm, resin wt: 5 mg, solution volume: 1 mL, ^{99}Tc concentration: tracer level.

3.2. Effect of equilibration time

To determine the time required to reach the extraction equilibrium, kinetic experiments were carried out with all the selected resins at $\text{pH} = 7$. In this experiment, 10 mg of the resins were taken along with 10 mL ^{99}Tc containing solution in a 15 mL plastic vial and rotated at 50 rpm using a tube rotator up to 132 hours. The results are graphically represented in Fig. 2 (k_d vs. time) and Fig. S1 as % extraction, which indicates that the extraction is completed within 4 hours of equilibration time for most of the resins except resin 830 and 890. While for resin 830, equilibrium was reached at ~ 48 hours, continuous increase in K_d was observed for resin 890 even after 132 hours of equilibrium. This may be due to the weak base anion exchange type of resin for 890, where free base tertiary amine functional groups take some time to be protonated and become active for ion-exchange.^{31,32} Though it requires long time to reach equilibrium, the K_d value was observed to be highest among all the resins tested in the present study. The four hour equilibration time for the resins 820, 810, 300 and 930 shows kinetically better performance than

many commercially available established resins for ^{99}Tc such as Purolite A-850/A-520E, Amberlite IRA-900/904, Reillex HPQ, Sybron Ionac SR-6/7 etc. These resins exhibit much higher equilibrium time (25 hr or more) than the resins under present study.²⁸ This signifies that, the resins under present study are practically more suitable for plant scale applications where time constraint is an important factor like column operation or rapid separation for analytical purpose.

From the comparative results, it can be noted that, the uptake capacity of resin 930 is least which may be due to the different polymeric backbone (polyacrylic based) as compared to other resins which are originated from styrene based polymeric support. The inferior performance of 930 resin with respect to the other resins also may be due to the lower total anion exchange capacity (0.8 mequiv/ml of dry resin) of the former or poor diffusivity of TcO_4^- ions through polyacrylate-divinylbenzene resin matrix. Resin 300 showed next higher loading capacity, which is least among all styrene based resins used in the present study. This can be explained on the basis of ionic diffusion into the bulk material. Resin 300 has gel type morphology where as all other resins are of macroreticular type beads. The gel-type morphology probably hinders the TcO_4^- anion to reach the bulk of the beads. On the other hand, TcO_4^- anion can easily be diffused through the bulk of the other resins and resulted in higher loading capacity. Among all macroreticular type, strong base resins, 810 shows highest capacity probably due to higher total exchange capacity (1.0 meq/mL) compared to other resins. The table 2 represents the value of K_d and K_d^{Eq} for all the resins after 4 hours and 132 hours of equilibration.

Table 2. K_d and K_d^{Eq} values of the resins after 4 h and 132 h

Resin	Total anion exchange capacity (mequiv/g)	K_d (mL/g) (4 h)	K_d^{Eq} (mL/mequiv) (4 h)	K_d (mL/g) (132 h)	K_d^{Eq} (mL/mequiv) (132 h)
810	1.6	118253.2	73908.2	118255.5	73909.7
820	1.8	80208.0	44560.0	115654.7	64252.5
830	1.6	44879.5	28049.5	86997.5	54373.5
300	2.1	39503.1	18811.0	39505.8	18812.3
890	2.5	28895.0	11558.0	195018.0	78007.0
930	1.34	1805.1	1347.0	1809.2	1350.1

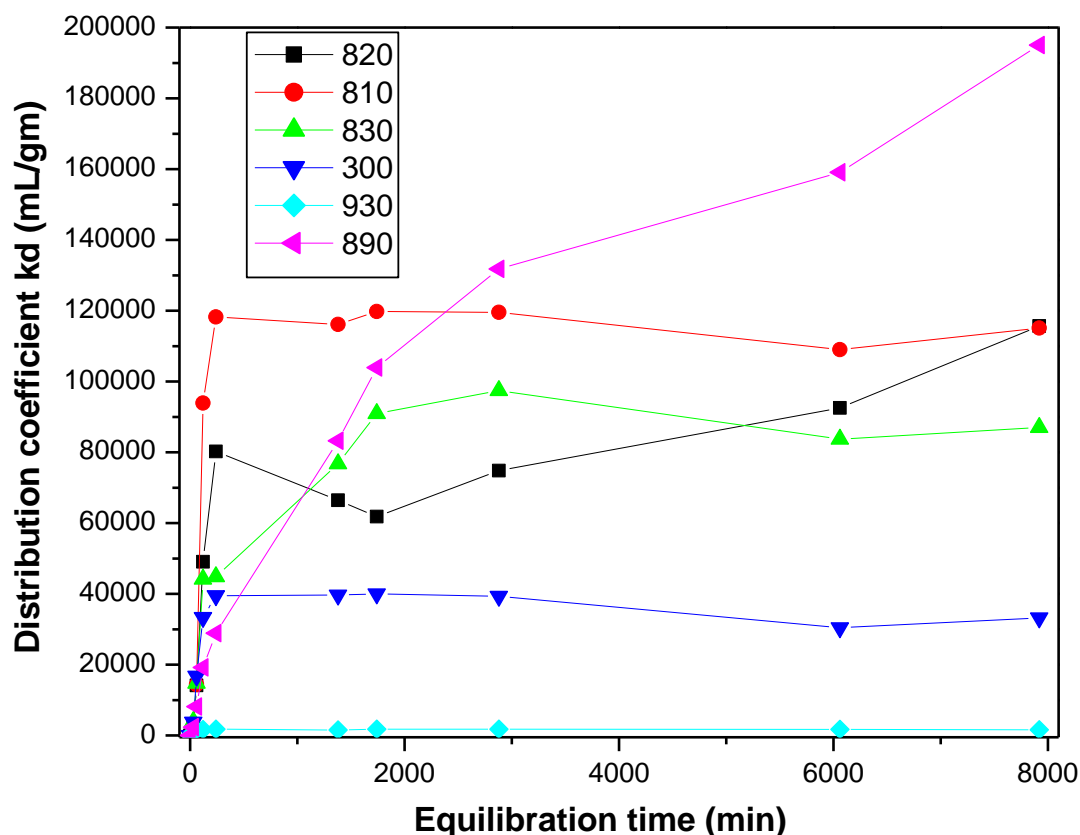


Figure 2. Effect of contact time; pH = 7, rotation: 50 rpm, resin wt: 10 mg, solution volume: 10 mL, ^{99}Tc concentration: tracer level.

3.3. Effect of concentration

The relation between the equilibrium concentration of the solute in the aqueous solution and the adsorbed quantity is very important to understanding the sorption behavior and to find out the optimized sorption conditions. Experiments were conducted with 1mL solutions having initial ReO_4^- concentration varying from 5 mg/L to 2500 mg/L and a fixed mass of resin (5 mg) with 4 h equilibration to investigate the effect of initial ReO_4^- concentration on the adsorption onto the resins. Fig. 3 exhibits the amount of adsorbed ReO_4^- versus the equilibrium concentrations of ReO_4^- . As expected the adsorption capacity increased with the equilibrium metal concentration. With more ReO_4^- present in solution, larger fraction of the active sites is involved in the adsorption process. The steep slope of the plots is a desirable feature of the sorption system and this indicates that these resins act as very efficient adsorbent for ReO_4^- . It can also be observed that, the resins 300, 810 and 820 have comparatively higher capacity with respect to resin 890 and 930. The weak base property of resin 890 which attends equilibrium at longer time and resin

930 which has least TEC (0.8 meq/ml) and polyacrylic backbone may be responsible for their relatively poor uptake capacity.

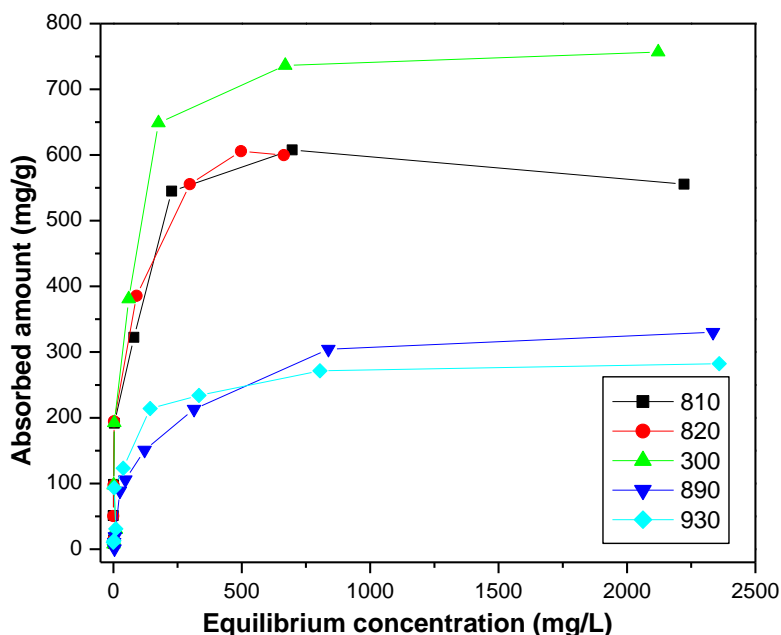


Figure 3. Effect of concentration; pH = 7, contact time: 4 h, rotation: 50 rpm, resin wt: 5 mg, solution volume: 1 mL, ⁹⁹Tc concentration: tracer level.

3.3.1. Langmuir sorption isotherm

The Langmuir isotherm can be described for a system for which solid adsorbent has limited adsorption capacity q_{\max} , one adsorption site adsorbs one molecule/ion, all adsorption sites are equivalent/similar, the sites are sterically and energetically independent on the adsorbed amount, adsorption onto the solid surface is monolayer in nature. The Langmuir sorption isotherm can be presented mathematically as,^{33,34}

$$\frac{C_{\text{eq}}}{q} = \frac{1}{bq_{\max}} + \frac{C_{\text{eq}}}{q_{\max}} \quad \dots\dots (2)$$

Where, C_{eq} represent the equilibrium concentration of ReO_4^- ion in the aqueous phase, 'q' gives the amount of ReO_4^- sorbed on the resins at equilibrium, ' q_{\max} ' and 'b' signify the maximum amount of ReO_4^- sorbed at saturation and the sorption coefficient ($\text{L}\cdot\text{mg}^{-1}$) respectively. The experimental data of ReO_4^- adsorption on the resins was fitted in the linear equation (Eq. (2)) and various isotherm parameters were derived from the straight line plot of the Langmuir sorption isotherm. The values of q_{\max} and b obtained from the liner plots were mentioned in table 3 for the resins under present study. Hall et al. have suggested that, the adsorption process can be favorable if the value of the Langmuir constant 'b' lies between 0 and 1.³⁵ The values of sorption

coefficient in the present system between 0-1 suggest favorable sorption of the ReO_4^- ion onto the selected resins. The fairly good fitting of the experimental data (R^2) to the Langmuir isotherm also signifies monolayer sorption of ReO_4^- onto the resin surfaces.

3.3.2. Freundlich sorption isotherm

The sorption experimental data were also fitted with the Freundlich isotherm model according to the following Eq. (3).

$$\log \frac{x}{m} = \log K_f + \frac{1}{n} \log C_{eq} \dots\dots (3)$$

This Freundlich isotherm considers multilayer sorption of any species onto a solid surface.^{36,37} ‘ C_{eq} ’ is the equilibrium concentration of ReO_4^- , ‘ x/m ’ indicates the concentration of ReO_4^- ions per unit mass of the resins. ‘ K_f ’ is a constant which depends on the sorption capacity and ‘ n ’ is related to the metal sorption intensity. For the Freundlich isotherm, the value of $1/n$ lies between 0 and 1.

The experimental data of ReO_4^- uptake by the resins were plotted in the linear form of the Freundlich sorption isotherm ($\log q_e$ vs $\log C_{eq}$). The poor fitting of the data points suggest that, the present ion-exchange process for ReO_4^- ions does not follow the Freundlich isotherm. This indicates the absence of multilayer sorption of perrhenate onto the resins which in turn supports the monolayer type of adsorption (vide supra: Langmuir isotherm). The parameters obtained from different isotherm fitting are listed in Table 3.

Table 3. Parameters obtained from Langmuir and Freundlich isotherm plots

Isotherm	Resins	Plot	Parameters
Langmuir	810	C_e/q_e vs C_e	$q_{\max} = 564.97 \pm 9.63$ mg/g, $b = 0.06 \pm 0.02$ L/mg, $R^2 = 0.998$
	820		$q_{\max} = 617.28 \pm 18.57$ mg/g, $b = 0.05 \pm 0.02$ L/mg, $R^2 = 0.994$
	300		$q_{\max} = 775.19 \pm 14.67$ mg/g, $b = 0.02 \pm 0.01$ L/mg, $R^2 = 0.998$
	890		$q_{\max} = 347.22 \pm 7.26$ mg/g, $b = 0.008 \pm 0.002$ L/mg, $R^2 = 0.998$
	930		$q_{\max} = 343.64 \pm 5.36$ mg/g, $b = 0.02 \pm 0.01$ L/mg, $R^2 = 0.994$
Freundlich	810	$\log q_e$ vs $\log C_e$	$\text{Log } K_f = 3.64 \pm 0.21$, $n = 2.27 \pm 0.24$, $R^2 = 0.9561$
	820		$\text{Log } K_f = 3.60 \pm 0.25$, $n = 2.10 \pm 0.25$, $R^2 = 0.9435$
	300		$\text{Log } K_f = 3.11 \pm 0.29$, $n = 1.74 \pm 0.19$, $R^2 = 0.9499$
	890		$\text{Log } K_f = 1.78 \pm 0.36$, $n = 1.65 \pm 0.19$, $R^2 = 0.9451$
	930		$\text{Log } K_f = 2.58 \pm 0.24$, $n = 2.04 \pm 0.20$, $R^2 = 0.9617$

3.4. Desorption studies

To check the feasibility for reusing the resins towards pertechnetate uptake for multiple cycles, the loaded resins were equilibrated with different reagent solutions (4M NaCl, 4M NaNO₃, 4M HNO₃, and 4M HCl) for desorption purpose. It can help not only to minimize the secondary waste generation during decontamination cycle, but also to use the sorbent materials in optimum way. Figure 4 indicates the desorption results for two types of resins (300 and 820) for two different contact times. It can be observed that, with 4M HNO₃ maximum (more than 98%) desorption is possible, followed by 4M NaNO₃ (30-35 %), 4M HCl (20-25 %), and 4M NaCl (15-20 %). This signifies that, NO₃⁻ ions more efficiently replace TcO₄⁻ ions from the resins than Cl⁻ ion. It can also be noticed that, no additional desorption proceeds after 5 h of contact time which is almost similar even up to 18 h. Therefore, desorption kinetics also follow similar trend as loading kinetics (vide supra, Fig. 2). The desorption also has negligible dependence on resin morphology (gel type 300 vs macroreticular 820). This result indicates the possibility for reusing the resins towards TcO₄⁻ uptake for multiple cycles.

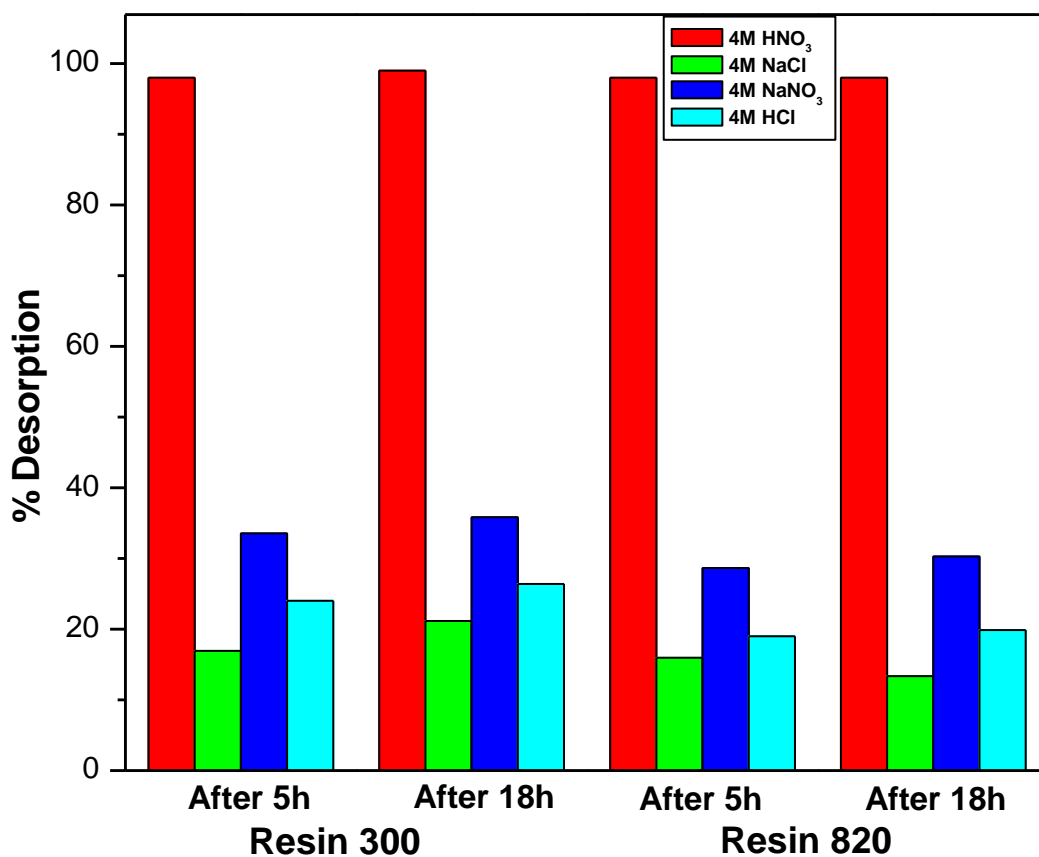


Figure 4. Comparison of ^{99}Tc desorption from loaded resins with different reagents viz, 4M NaCl, 4M NaNO_3 , 4M HNO_3 , and 4M HCl; contact time: 5 h, rotation: 50 rpm, loaded resin wt: 10 mg, reagent volume: 1 mL.

3.5. Equilibration studies with irradiated resins

The resin samples were irradiated inside a gamma chamber with known gamma ray dose rate (kGy/h), to check the possibility of reusing the resins multiple cycles. During their usage for multiple cycles, the resins may get deteriorated due to radiation damage. The radiation may break the polymeric chain responsible for the structural rigidity or damage/modify the functional groups of the resin and change the overall ion-exchange properties of the resins.^{38,39}

5 g of each resin was exposed in a gamma chamber for different time periods to irradiate the resins with total absorbed dose of 250, 500, and 1000 kGy. The resins turned light to dark yellow after irradiation inside the chamber. The resins were then equilibrated with 1 mL tracer solution with the standard conditions optimized earlier. The Figure 5 indicates the effect of radiation dose on the resins separately and compared with the resin samples without irradiation (unirradiated). It can be noted that, the ^{99}Tc uptake capacities of the resins are reduced in a significant amount in case of styrene-divinyl benzene based resins. For polyacrylic acid based resin 930, the resin is found to be less radiation sensitive, which is reflected by its comparable uptake of ^{99}Tc as unirradiated resin. It is also noticeable that, with increasing total absorbed dose, the loading capacity is continuously reduced as expected (highest reduction in loading capacity was found for 810 and 820). The results infer that, these resins are very sensitive towards radiation and therefore not suitable for multiple cycle operation. However, the soft beta emission ($\beta_{\text{max}} = 294$ keV) and long half-life (2.11×10^5 years) of ^{99}Tc yield very low dose rate which can't reduce the resin capacity in a significant level.

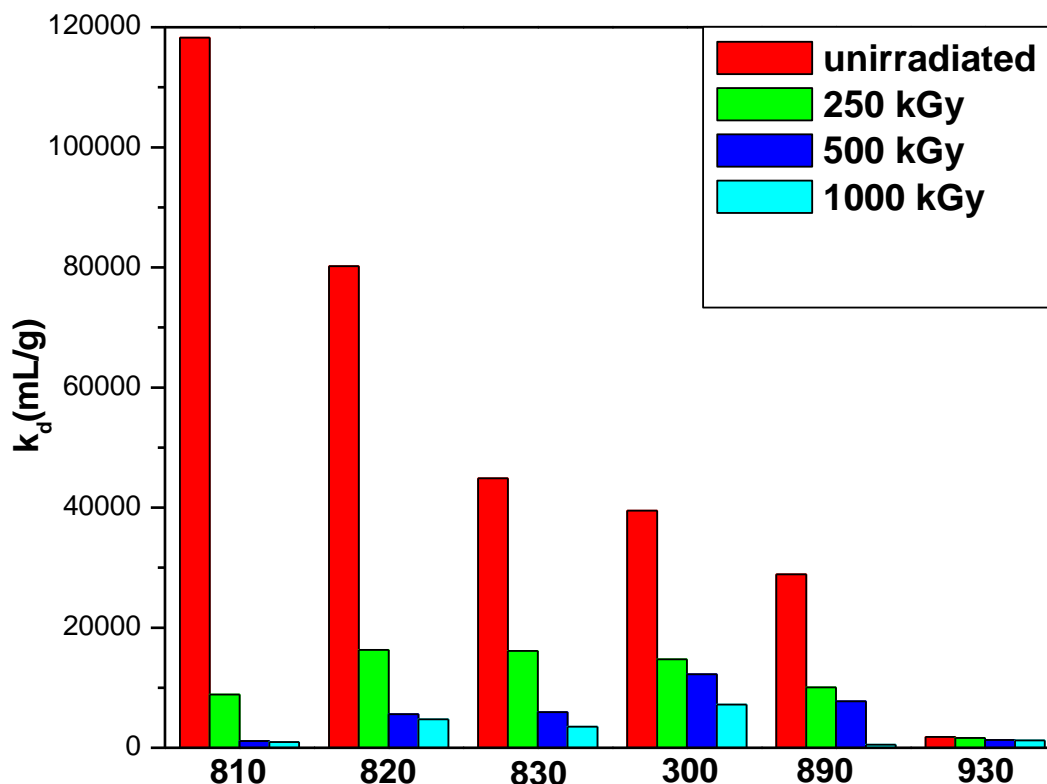


Figure 5. Comparison of γ -dose effect on ^{99}Tc uptake by the resins; contact time: 5 h, rotation: 50 rpm, loaded resin wt: 10 mg, reagent volume: 1 mL.

3.6. SEM of the resins

The scanning electron microscopic analysis is used to investigate the size, shape and morphology of any material which helps to determine the qualitative properties of sorption and compare among the adsorbents.^{40,41} For this purpose, two resins 300 and 830 have been selected for having gel type and macroporous structure of the beads respectively. The SEM image of 300 resin (Figure 6a) shows that, it is spherical in shape with a diameter of 520 μm . The surface of the beads is smooth throughout except in few places where some surface roughness has been observed with 2-5 μm length. On the other hand, The SEM image of 830 resin (Figure 6c) exhibits that, it is also spherical in nature with a diameter of 470 μm . Here the surface is not smooth as resin 300 and surface roughness is observed randomly of maximum 10 μm length throughout the resin. There is no significant change observed in SEM image (Figure 6b) for resin 300 after ReO_4^- adsorption. The size and shape was intact after 4 hours of equilibration (optimized contact time) and no swelling or deformation was observed after Re sorption. The surface was equally smooth before and after sorption process. For resin 830, the surface become

more rough (Figure 6d) after Re adsorption and some aberrations have been observed throughout the bead.

The EDS plot of resin 300 after Re adsorption (Figure 7a) indicates that, different L-series X-rays of Re are present in the plot along with K-series X-rays of C, O and Cl and confirms uptake of Re by the resin beads. The atomic and weight percentage of Re after sorption process are 0.45 and 5.5% respectively (Table S1). Similar observation was observed in case of resin 830 (Figure 7b). However, the atomic and weight percentage of Re after sorption process are 0.38 and 5.1% respectively (Table S2). The lower Re% on the resin bead for 830 compared to resin 300 is may be due to diffusion of Re into the resin bulk for 830 (macroreticular) as compared to resin 300 (gel type).

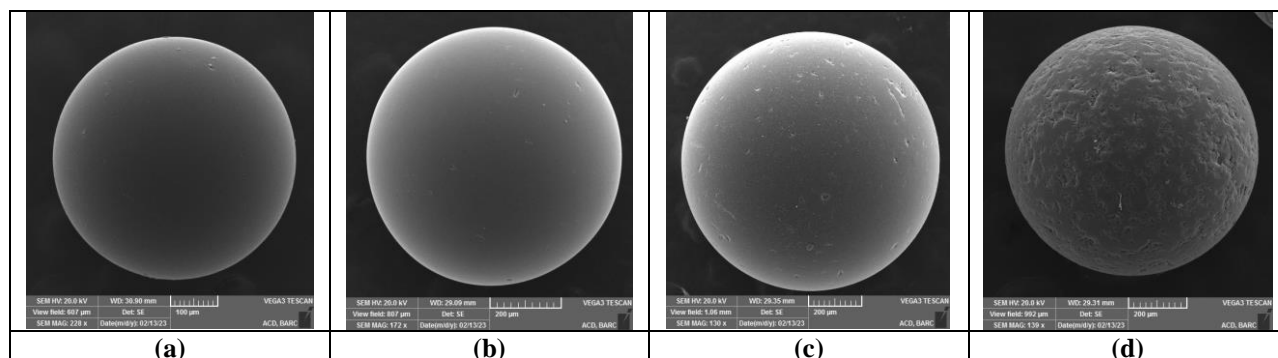


Figure 6. SEM images of fresh (a:300, c:830) and loaded (a:300, c:830) resins

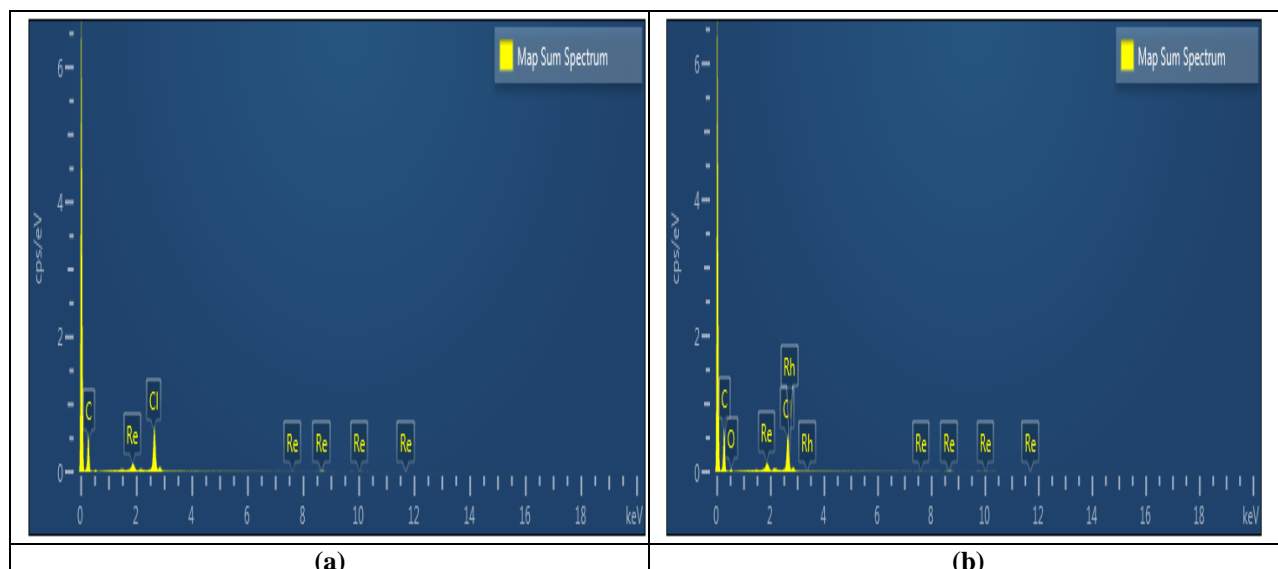
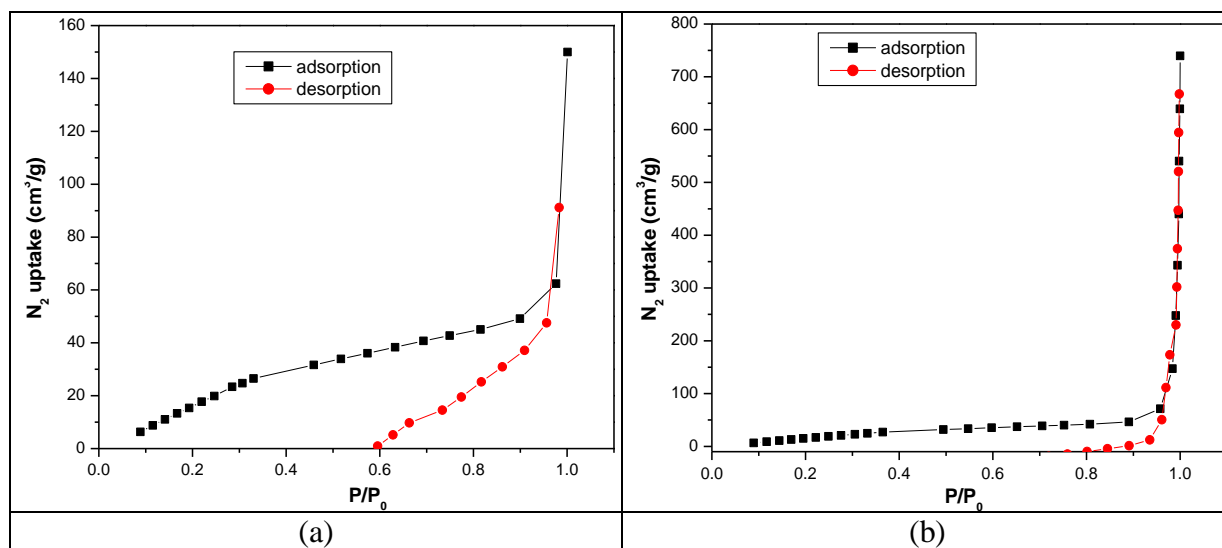


Figure 7. EDS spectra of loaded (a:300, b:830) resins

3.7. BET analysis

To get the idea about porosity and pore sizes of the anion exchange resins, nitrogen adsorption measurement experiment was carried out at 77K. As shown in Figure 8, very slow increment in gas uptake is found at lower pressure (P/P_0) in the nitrogen adsorption-desorption isotherms of all the resins, which suggests that the resins don't have microporous structure rather may have macroporous networks.⁴² Type-II reversible adsorption isotherm model is observed for all the cases indicate unrestricted monolayer-multilayer adsorption of N_2 molecules, which is true for either non-porous or macroporous sorbent.^{43,44} The measured Brunauer-Emmett-Teller (BET) surface area of the resins is in the range of 123-218 m^2/g . Resin 930 with polyacrylate-divinylbenzene polymeric backbone have the highest specific surface area (218 m^2/g). Low BET surface area of the resins most likely resulted from the low crystallinity (polymeric in nature) of the beads and presence of counter anion Cl^- inside the pore channels.⁴⁵ The pore size distribution plots for the resins are shown in Fig. S2-S6. This is the plot of pore diameter (\AA) versus relative pore volume (cm^3/g), which can provide the idea of average pore size of the resins. The plots indicate that, the dominant pore diameter of the resins is $\sim 20-25 \text{\AA}$ except resin 890 for which it is observed to be 420\AA . The pores are much larger than the hydrodynamic diameter of TcO_4^- (2.5 \AA) or ReO_4^- (2.6 \AA), which allows the effective anion transfer within the pores.⁴⁶



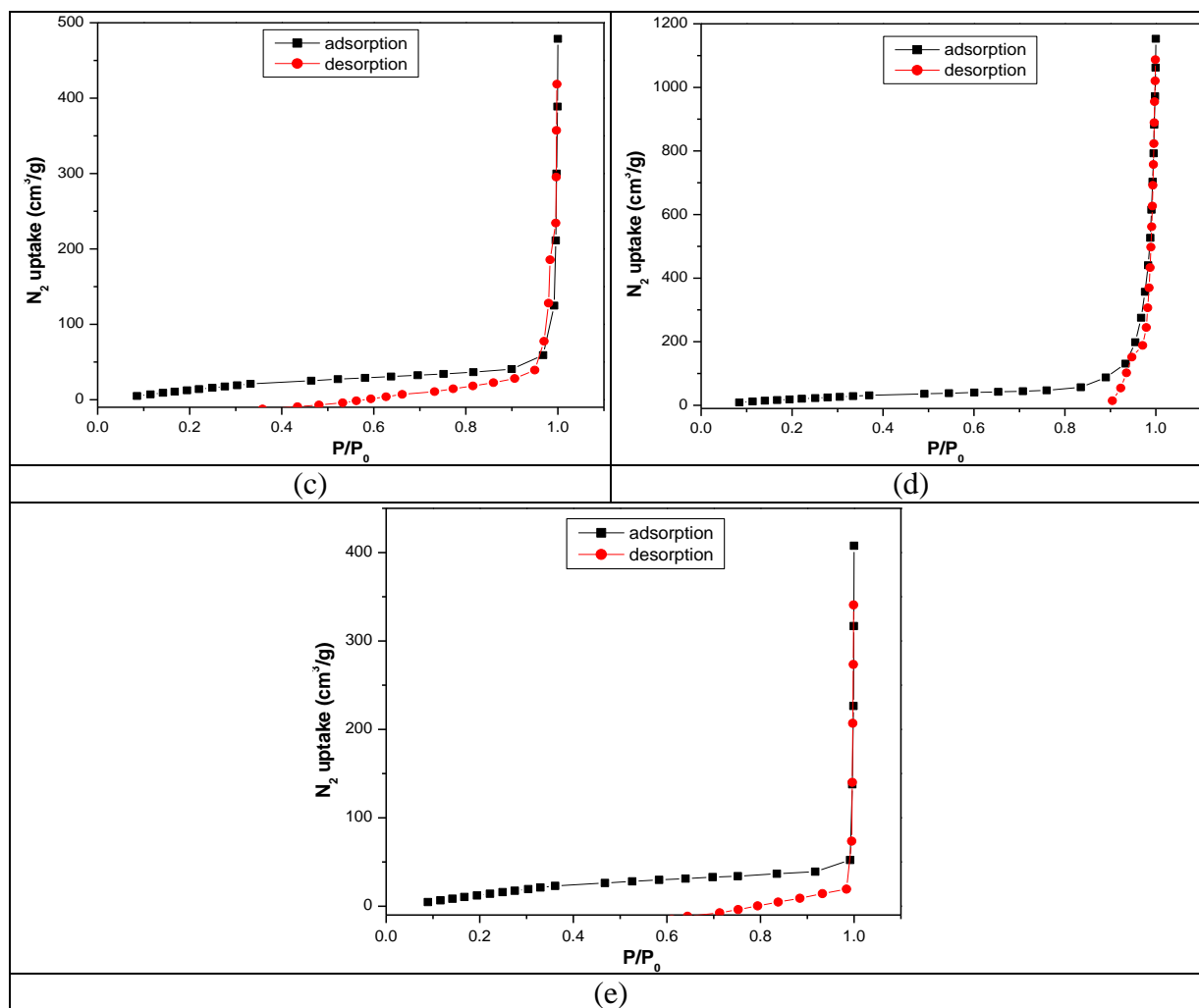


Figure 8. Nitrogen sorption isotherms (BET experiment) for resin a) 810, b) 820, c) 830, d) 890, and e) 930.

3.8. XPS analysis

X-ray photoelectron spectroscopy is a very useful technique for the determination of elemental composition and their oxidation states of any matrix. To check the Re uptake property by the resins, XPS analyses of the resin beads have been carried out before and after equilibration with ReO_4^- bearing aqueous solution. 830 and 890 resins were selected as the representatives of the strong base and weak base anion exchanger respectively.

XPS spectrum of resin 830 before contacting with Re containing solution exhibits characteristic binding energy peaks of O1s, C1s, N1s and Cl2p (Fig. 9a). This confirms that this resin is in ionic form with Cl^- as counter anion (quaternary ammonium form). The additional peak at ~ 46 eV is observed when the resin was equilibrated with ReO_4^- solution (Fig. 9b). This can be assigned as Re4f binding energy peak, when Re is present is +7 oxidation state (ReO_4^- here).^{44,47}

To further verify the roles of quaternary ammonium groups in the adsorption process of ReO_4^- , the N1s core-level spectra of 830 and 890 with ReO_4^- were analyzed. The N1s core level of $+\text{NR}_4^-$ (401.0 eV) is shifted to lower binding energy after ReO_4^- loading (400.5 eV). This can be explained on the basis of the better charge neutralization (stronger interaction) of $+\text{NR}_4^-$ group in case of Re loaded 830 resin than the original Cl^- loaded resin. These results confirm the interactions between quaternary ammonium groups and ReO_4^- . The overlaid XPS spectra of 830 and 830- ReO_4^- indicate the occurrence of anion exchange process as the original peak of Cl2p is slightly diminished and a new peak of Re4f is appeared in 830- ReO_4^- . As the equilibration time for the preparation of equilibrated beads was kept 2 hour, therefore complete exchange of Cl^- anion with ReO_4^- was not observed. In case of 890 resin (weak base), 2 h contact time was found as very negligible time to reach equilibrium, no measurable amount of Re was loaded into the resin bead (absence of Re4f peak). Therefore, the XPS results also support very slow kinetics of resin 890 (vide supra). Missing of Cl2p peak in case of 890 spectrum also indicates free base type of resin (weak base).

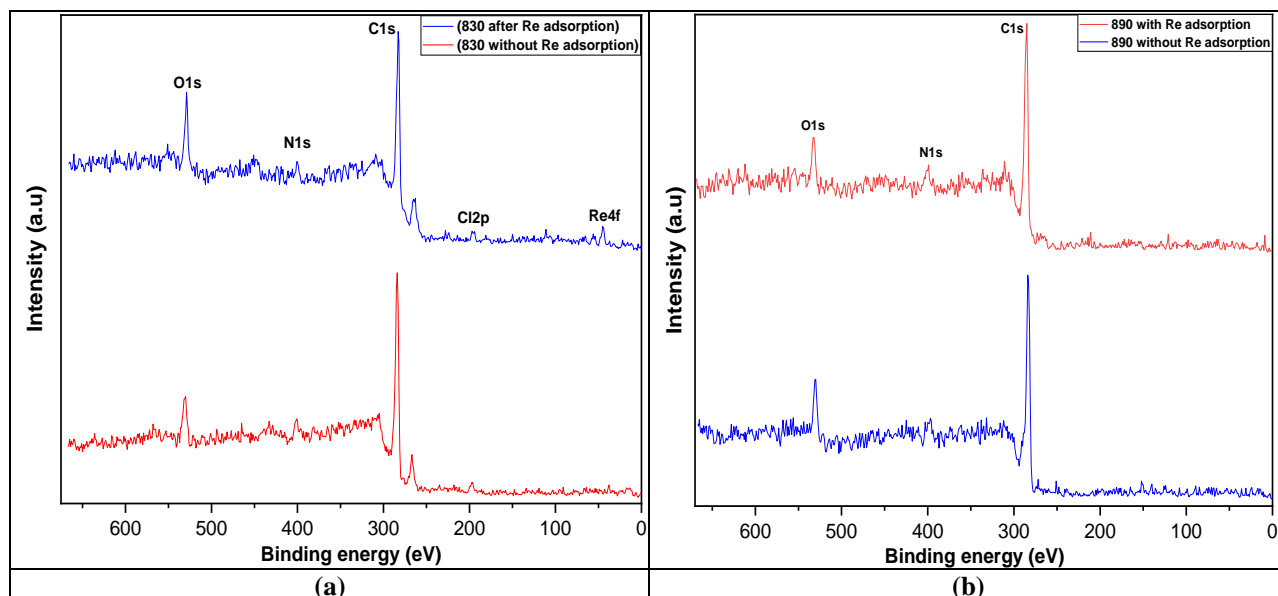


Figure 9. XPS spectra of the resins before and after ReO_4^- contact, a) 830, b) 890.

3.9. Thermogravimetric analysis

TG analysis has been carried out to determine the thermal stability of the resin beads. The TG plots for the resins were plotted in figure 10. It was observed during the initial tests that, all the resins loss a significant amount of mass (even up to 50%) when heated at 100-150°C temperature. This is consistent of the product specification data provided by the vendors as these

resins contain 48-72% moisture at room temperature. Therefore, TG analyses of these resins were conducted by setting the starting temperature at 300°C to ensure all moisture content in the resins were fully removed before observing actual temperature effect on the resins. It is evident that, the resins loss their weight in four to five steps. Up to 350°C, there is a slow reduction of weight and overall weight loss is ~5% for all resins. When the resins were heated up to 450°C, the rate of weight loss is very sharp with average weight loss of 50%. This may be attributed to the loss of amine functional groups at this temperature. Above 500°C all the resins loss their weight in multiple steps with varying rate of loss, which can be correlated with structural degradation of the basic resin backbone. In the last step at 775°C, no residual mass was left for any resin. This is in consistent with any organic resin which degrades completely at this high temperature. From the TG analyses it can be concluded that, all the resins are thermally stable up to 350°C, which can be appropriate for using these resin for high working temperature required for nuclear waste treatment.

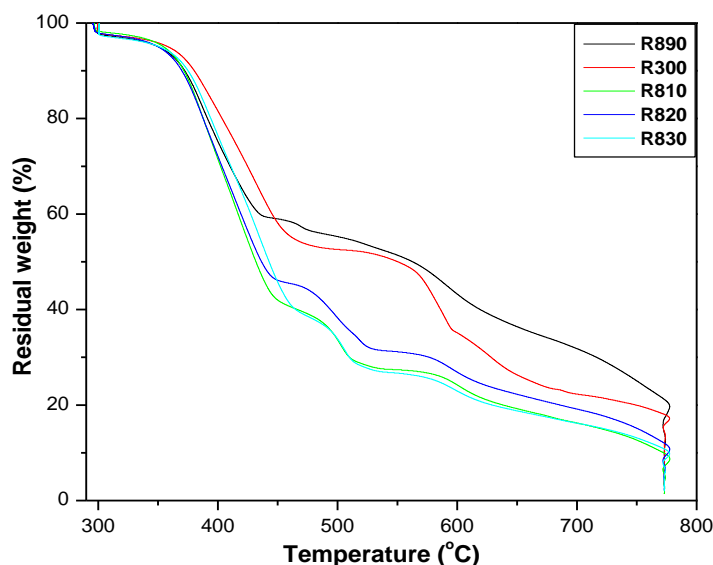


Figure 10. TGA plots of resin 810, 820, 830, 300, and 890.

3.10. Competition with common anions

Bianionic competition experiment was conducted to check the selectivity of the resins towards TcO_4^- separation. With this aim, uptake experiments were conducted taking TcO_4^- along with some common anions generally found in the ground water and soil. The selected anions are Cl^- and NO_3^- as monoanions, SO_4^{2-} and CO_3^{2-} as dianions, and PO_4^{3-} as trianion. In this experiment, the ratio of molar concentration of TcO_4^- and the other anions was kept as 1:1, 1:10, 1:100, 1:1000, and 1:10000. The results with NO_3^- competition are shown in figure 11. It can be noted

from the figure that, with increase in molar concentration ratio of NO_3^- ion, the removal % of TcO_4^- from the bianionic mixture is reduced as expected.^{21,48-49} However, even at 1:10000 molar ratio, the removal of TcO_4^- was found to be more than 60% in all cases, indicating the selectivity of the resins towards TcO_4^- ion. At 1:1, 1:10, and 1:100 molar ratio, virtually complete separation (~100 %) of TcO_4^- was observed with all the resins tested. Similar results are observed in case of Cl^- , SO_4^{2-} , CO_3^{2-} , PO_4^{3-} competitions. The selectivity towards TcO_4^- can be explained on the basis of hydration energy and hydrated volume of the anions used in this experiment. TcO_4^- being a bulky anion has least hydrated volume and minimum hydration energy (also due to monoanion). Therefore, after surpassing the hydration energy TcO_4^- can most conveniently be extracted in the solid phase from the aqueous medium compared to the other competition anions.

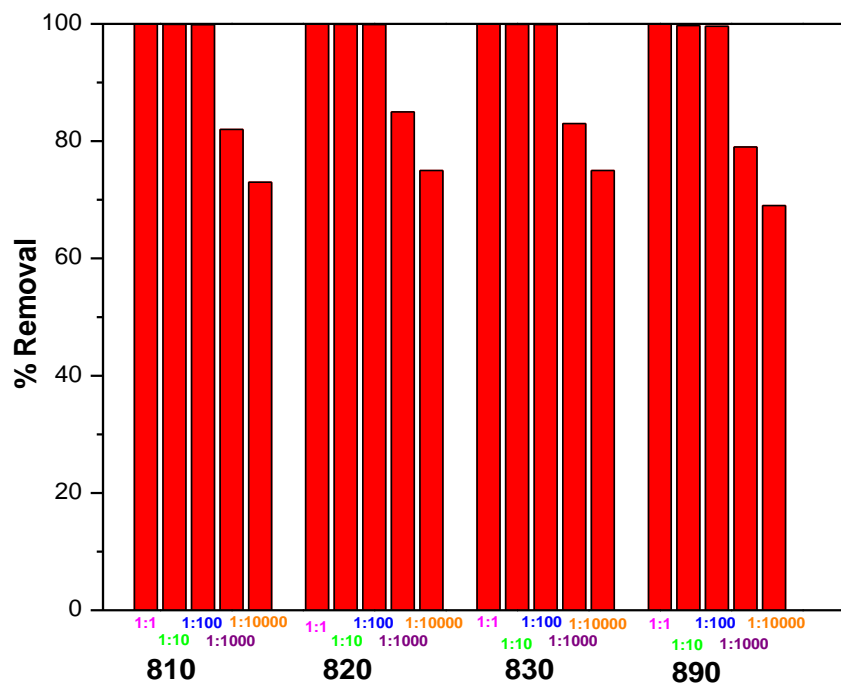


Figure 11. Bianionic uptake competition of TcO_4^- with NO_3^- .

3.11. FTIR analysis

FTIR analysis is extensively used for the characterization of materials with respect to the functional groups present. To check the nature of functional groups in the resin matrix, we have crushed the resins on an agate mortar and pestle for the analysis of these resins using FTIR in attenuated total reflectance (ATR) mode. The FTIR spectra of original resin samples and the resins after equilibration with ReO_4^- are given in figure 12 respectively. It can be noted from the spectra that, the broad peaks near to 3300 cm^{-1} is due to $-\text{OH}$ stretching frequency of water

molecules present within the resins as supplied. The peaks near about 1627 cm^{-1} , 1550 cm^{-1} , and 1475 cm^{-1} can be attributed to the aromatic C=C stretching, C=C bending, and C-H bending of methylene groups respectively. In case of post equilibrated resins with NH_4ReO_4 , the additional peak at 905 cm^{-1} was observed which can be ascertained as Re=O stretching frequency of ReO_4^- .^{21,44,48} Therefore, FTIR analyses provide direct evidence of Re loading onto the resin surface in the form of ReO_4^- .

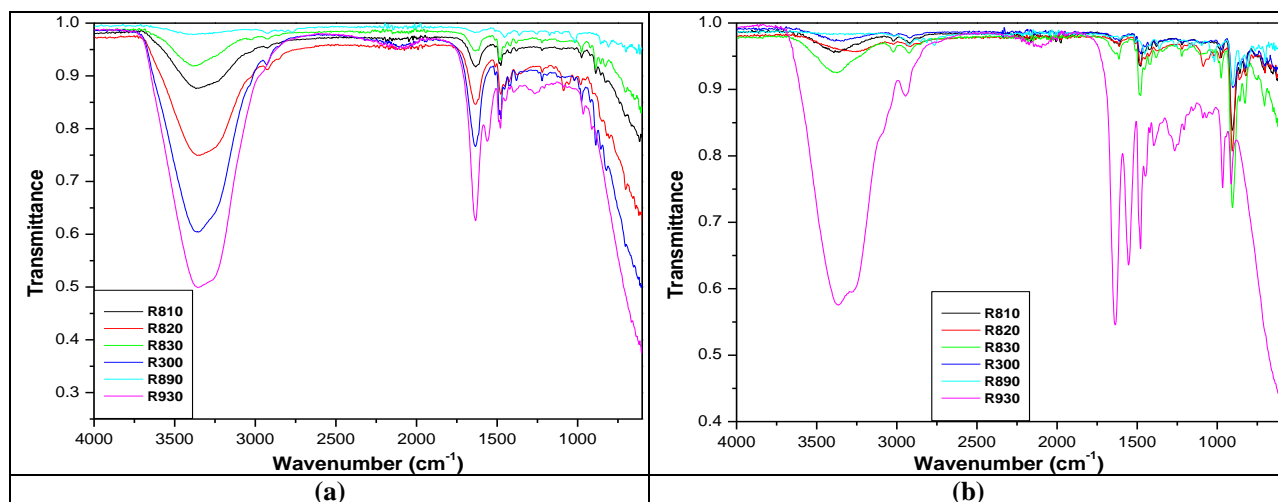


Figure 12. FTIR spectra of resin 810, 820, 830, 300, 890, and 300 (a) before and (b) after equilibration of ReO_4^- solution.

3.12. Thermodynamic studies

Thermodynamic studies are beneficial for understanding the effect of temperature on the adsorption equilibrium. For endothermic reactions, the reactions are more feasible at higher temperature where as the opposite effect is true for the exothermic reactions. From the Van't Hoff plot ($\ln K_{eq}$ vs $1/T$), some of the crucial thermodynamical parameters like Gibb's free energy change (ΔG), enthalpy change (ΔH), entropy change (ΔS) of the adsorption process can be obtained according to the following equations,

$$\Delta G = -RT \ln K_{eq} \dots (4)$$

$$\Delta G = \Delta H - T\Delta S \dots (5)$$

From the equations,

$$\begin{aligned} -RT \ln K_{eq} &= \Delta H - T\Delta S \\ \ln K_{eq} &= -\Delta H/RT + \Delta S/R \dots (6) \end{aligned}$$

The sorption experiments were carried out with resin 300 at different temperatures (25°C, 35°C, 45°C, and 55°C), and K_{eq} values have been calculated at each temperature using the following equation:

$$K_{eq} = I - \frac{F}{A} \dots (7)$$

Where, I and F are the initial and final concentration of ReO_4^- in aqueous solutions. The plot of K_{eq} versus $1/T$ is plotted and shown in figure 13. From the intercept and slope of the Van't Hoff plot, the values of change in enthalpy (ΔH), and change in entropy (ΔS) of the adsorption process is computed and the Gibb's free energy change (ΔG) is obtained from equation 5. The value of ΔH , ΔS , and ΔG is found to be 23.86 kJ/mol, 84.18 J/mol-K, and 1.39 kJ/mol respectively at 300 K. The negative value of ΔG indicates the feasibility and spontaneous nature of the ReO_4^- adsorption process onto the resin. The value of ΔH is observed to be positive which suggests that the adsorption process is endothermic in nature.

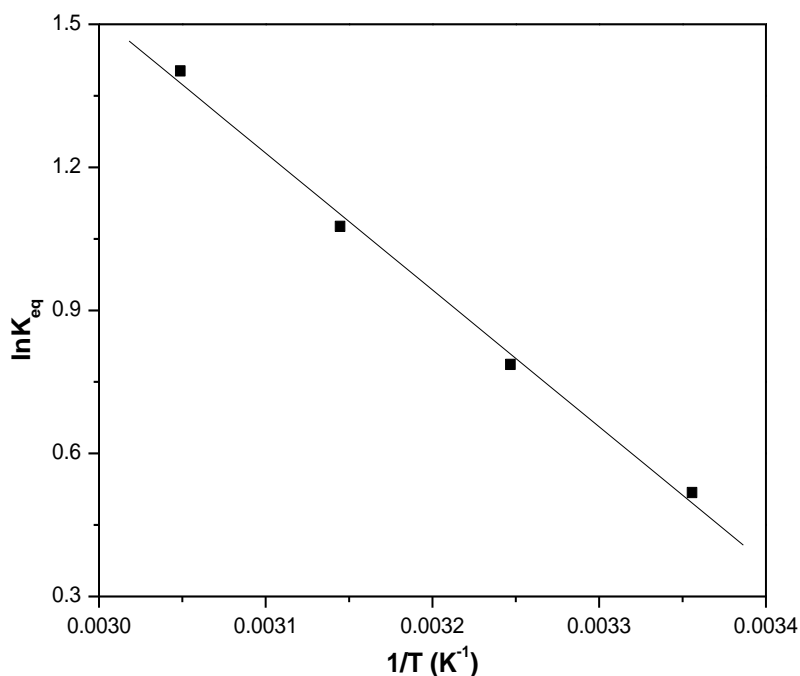


Figure 13. Van't Hoff plot of resin 300 at different temperatures.

4. CONCLUSIONS

The present study reveals that, styrene-divinylbenzene based strong and weak base Indion resins 810, 820, 830, 300, 890 can efficiently sequester ^{99}Tc from low level liquid waste. These resins perform much better than polyacrylic-divinylbenzene based strong base resin 930 in all aspects. Some of the resins were found to show better results than few ^{99}Tc specific resins like Purolite

A-850, Reillex HPQ, Amberlite IRA-900, Amberlite IRA-904, Purolite A-520E, Sybron Ionac SR-7, Sybron Ionac SR-6 well established earlier. These resins show good uptake capacities and better kinetic performance compared to many commercial and synthesized resins tested for this purpose. These resins can be used for multiple cycles after effectively remove loaded ^{99}Tc applying 4M HNO_3 , although these are found to be radiation sensitive particularly at high absorbed dose (many cycles can be performed due to low beta energy of ^{99}Tc). The resins before and after equilibration are characterized by BET, SEM, EDS, XPS, TG, and FTIR spectroscopy which confirm their ^{99}Tc uptake feasibility and adsorption mechanism is governed by purely ion-exchange type. Competition studies with most common anions found in ground water as well as soil like Cl^- , NO_3^- , SO_4^{2-} , CO_3^{2-} , PO_4^{3-} indicate that, even in presence of high concentration (1:10000 molar ratio) of these interfering anions, ^{99}Tc can be selectively removed by the resins confirming their effectiveness towards the decontamination of contaminated ground water with respect to ^{99}Tc .

AUTHOR INFORMATION

Corresponding Author

Debasish Das – Waste Management Division, Bhabha Atomic Research Centre, Trombay, Mumbai-400085, India; orcid.org/0000-0001-8726-5885; Email: deba.chem@gmail.com, debads@barc.gov.in

Notes

The authors declare no competing financial interest.

ACKNOWLEDGEMENTS

DD wants to acknowledge Smt. Mamta Gautam, Shri Gulshan Kharkate, and Smt. Darshana Malich for their help during the experiments. DD is thankful to Dr. Hirakendu Basu, Dr. Soumitra Kar, Dr. Virendra Kumar, Dr. Chiranjit Nandi, Dr. V.G. Mishra, and Dr. R.K. Sharma for their various analytical supports at different stages of study. DD would also like to acknowledge Dr. A.S. Pente, Shri K.C. Pancholi, Shri Anand Gangadharan, and Smt. Smitha Manohar for their continuous support and encouragement for the work.

REFERENCES

- (1) Dresselhaus, M. S.; Thomas, I. L. Alternative energy technologies. *Nature*. 2001, 414, 332–337.

- (2) Adebayo, T. S.; Ozturk, I.; Ağa, M.; Uhunamure, S. E.; Kirikkaleli, D.; Shale, K. Role of natural gas and nuclear energy consumption in fostering environmental sustainability in India. *Sci Rep.* **2023**, *13*, 11030–11044.
- (3) Kappner, K.; Letmathe, P.; Weidinger, P. Causes and effects of the German energy transition in the context of environmental, societal, political, technological, and economic developments. *Energ Sustain Soc.* **2023**, *13*, 28–53.
- (4) Horvath, A., Rachlew, E. Nuclear power in the 21st century: Challenges and possibilities. *Ambio.* **2016**, *45*, 38–49.
- (5) Darab, J. G.; Amonette, A. B.; Burke, D. S. D.; Orr, R. D.; Ponder, S. M.; Schrick, B.; Mallouk, T. E.; Lukens, W. W.; Caulder, D. L.; Shuh D. K. Removal of pertechnetate from simulated nuclear waste streams using supported zerovalent iron. *Chem. Mater.* **2007**, *19*, 5703–5713.
- (6) Lee, M.-S.; Um, W.; Wang, G.; Kruger, A. A.; Lukens, W. W.; Rousseau, R.; Glezakou, V.-A. Impeding ⁹⁹Tc(IV) mobility in novel waste forms. *Nat. Commun.* **2016**, *7*, 12067–12072.
- (7) Drout, R. J.; Otake, K.; Howarth, A. J.; Islamoglu, T.; Zhu, L.; Xiao, C.; Wang, S.; Farha, O. K. Efficient capture of perrhenate and pertechnetate by a mesoporous Zr metal-organic framework and examination of anion binding motifs. *Chem. Mater.* **2018**, *30*, 1277–1284.
- (8) Rard, J. A.; Rand, M. H.; Anderegg, G.; Wanner, H. *Chemical Thermodynamics of Technetium*; North Holland, Elsevier: Amsterdam, The Netherlands, 1999; Vol. 3, p 543.
- (9) Banerjee, D.; Kim, D.; Schweiger, M. J.; Kruger, A. A.; Thallapally, P. K. Removal of TcO₄⁻ ions from solution: materials and future outlook. *Chem. Soc. Rev.* **2016**, *45*, 2724–2739.
- (10) Waage, N. K. M.; Morris, K.; Lloyd, J. R.; Shaw, S.; J. Mosselmans, F. W.; Boothman, C.; Bots, P.; Rizoulis, A.; Livens, F. R.; Law, G. T. W. Impacts of Repeated Redox Cycling on Technetium Mobility in the Environment. *Environ. Sci. Technol.* **2017**, *51*, 14301–14310.
- (11) Bond, A. H.; Gula, M. J.; Harvey, J. T.; Duffey, J. M.; Horwitz, E. P.; Griffin, S. T.; Rogers, R. D.; Collins, J. L. Flowsheet Feasibility Studies Using ABEC Resins for Removal of Pertechnetate from Nuclear Wastes. *Ind. Eng. Chem. Res.* **1999**, *38*, 1683–1689.
- (12) Katayev, E. A.; Kolesnikov, G. V.; Sessler, J. L. Molecular recognition of pertechnetate and perrhenate. *Chem. Soc. Rev.* **2009**, *38*, 1572–1586.
- (13) Beer, P. D.; Gale, P. A. Anion Recognition and Sensing: The State of the Art and Future Perspectives. *Angew. Chem., Int. Ed.* **2001**, *40*, 486–516.
- (14) Wang, Y.; Gao, H. Compositional and structural control on anion sorption capability of layered double hydroxides (LDHs). *J. Colloid Interface Sci.* **2006**, *301*, 19–26.
- (15) Goh, K. H.; Lim, T. T.; Dong, Z. Application of layered double hydroxides for removal of oxyanions: A review. *Water Res.* **2008**, *42*, 1343–1368.
- (16) Wang, S. A.; Alekseev, E. V.; Diwu, J.; Casey, W. H.; Phillips, B. L.; Depmeier, W.; Albrecht-Schmitt, T. E. NDTB-1: A Supertetrahedral Cationic Framework That Removes TcO₄⁻ from Solution. *Angew. Chem., Int. Ed.* **2010**, *49*, 1057–1060.
- (17) Cui, W. -R.; Xu, W.; Chen, Y. -R.; Liu, K.; Qiu, W. -B.; Li, Y.; Qiu, J. -D. Olefin-linked cationic covalent organic frameworks for efficient extraction of ReO₄⁻/⁹⁹TcO₄⁻. *J. Hazard. Mater.* **2023**, *446*, 130603.
- (18) Wang, Y.; Xie, M.; Lan, J.; Yuan, L.; Yu, J.; Li, J.; Peng, J.; Chai, Z.; Gibson, J. K.; Zhai, M.; Shi, W. Radiation Controllable Synthesis of Robust Covalent Organic Framework Conjugates for Efficient Dynamic Column Extraction of ⁹⁹TcO₄⁻. *Chem* **2020**, *6*, 2796–2809.

- (19) Custelcean, R. Urea-functionalized crystalline capsules for recognition and separation of tetrahedral oxoanions. *Chem. Commun.* **2013**, 49, 2173 – 2182.
- (20) Fei, H.; Bresler, M. R.; Oliver, S. R. J. A New Paradigm for Anion Trapping in High Capacity and Selectivity: Crystal-to-Crystal Transformation of Cationic Materials. *J. Am. Chem. Soc.* **2011**, 133, 11110 – 11113.
- (21) Sheng, D.; Zhu, L.; Xu, C.; Xiao, C.; Wang, Y.; Wang, Y.; Chen, L.; Diwu, J.; Chen, J.; Chai, Z.; Albrecht-Schmitt, T. E.; Wang, S. Efficient and Selective Uptake of TcO_4^- by a Cationic Metal-Organic Framework Material with Open Ag^+ Sites. *Environ. Sci. Technol.* **2017**, 51, 3471–3479.
- (22) Del Cul, G. D.; Bostick, W. D.; Trotter, D. R.; Osborne, P. E. Technetium-99 Removal from Process Solutions and Contaminated Groundwater. *Sep. Sci. Technol.* **1993**, 28, 551-564.
- (23) Ashley, K. R.; Ball, J. R.; Pinkerton, A. B.; Abney, K. D.; Norman, C. Sorption behavior of pertechnetate on reillex(tm)-HPQ anion exchange resin from nitric acid solution. *Solvent Extr. Ion. Exch.* **1994**, 12, 239-259.
- (24) Kawasaki, M.; Omori, T.; Hasegawa, K. Adsorption of Pertechnetate on an Anion Exchange Resin. *Radiochim. Acta* **1993**, 63, 53-56.
- (25) Ihsanullah. Optimization of Various Factors for the Separation of Technetium Using Anion-Exchange Resins. *Sep. Sci. Technol.* **1994**, 29, 239-247.
- (26) Ashley, K. R.; Ball, J. R.; Abney, K. D.; Turner, R.; Schroeder, N. C. Breakthrough volumes of TcO_4^- on Reillex™-HPQ anion exchange resin in a Hanford Double Shell Tank simulant. *J. Radioanal. Nucl. Chem.* **1995**, 194, 71-79.
- (27) Rogers, R. D.; Bond, A. H.; Griffen, S. T.; Horwitz, E. P. New Technologies for Metal Ion Separations: Aqueous Biphasic Extraction Chromatography (ABEC). Part I Uptake of Pertechnetate. *Solvent Extr. Ion Exch.* **1996**, 14, 919-946.
- (28) Bonnesen, P. V.; Brown, G. M.; Alexandratos, S. D.; Bavoux, L. B.; Presley, D. J.; Patel, V.; Ober, R.; Moyer, B. A. Development of Bifunctional Anion-Exchange Resins with Improved Selectivity and Sorptive Kinetics for Pertechnetate: Batch-Equilibrium Experiments. *Environ. Sci. Technol.* **2000**, 34, 3761–3766.
- (29) Alexandratos, S. D.; Brown, G. M.; Bonnesen, P. V.; Moyer, B. A. Bifunctional Anion-Exchange Resins with Improved Selectivity and Exchange Kinetics. U.S. Patent 6,059,975, May 9, 2000.
- (30) Gu, B.; Liang, L.; Brown, G. M.; Bonnesen, P. V.; Moyer, B. A.; Alexandratos, S. D.; Ober, R. *A Field Trial of Novel Bifunctional Resins for Removing Pertechnetate (TcO_4^-) from Contaminated Groundwater*; Report ORNL/TM-13593; Oak Ridge National Laboratory: Oak Ridge, TN, March 1998.
- (31) Miyazaki, Y.; Nakai, M. Protonation and ion exchange equilibria of weak base anion-exchange resins. *Talanta.* **2011**, 85, 1798–1804.
- (32) Kassar, C.; Graham, C.; Boyer, T. H. Removal of perfluoroalkyl acids and common drinking water contaminants by weak-base anion exchange resins: Impacts of solution pH and resin properties. *Water Res. X.* **2022**, 17, 100159.
- (33) Bessbousse, H.; Rhlalou, T.; Verchere, J.F.; Lebrun, L. Novel metal-complexing membrane containing poly(4-vinylpyridine) for removal of Hg(II) from aqueous solution. *J. Phys. Chem. B.* **2009**, 113, 8588–8598.

- (34) Limousin, G.; Gaudet, J.P.; Charlet, L.; Szenknect, S.; Barthes, V.; Krimissa, M. Sorption isotherms: a review on physical bases, modeling and measurement. *Appl. Geochem.* **2007**, *22*, 249–275.
- (35) Hall, K.R.; Eagleton, L.C.; Acrivos, A.; Vermeulen, T. Pore- and solid-diffusion kinetics in fixed-bed adsorption under constant-pattern conditions, *Ind. Eng. Chem. Fundam.* **1966**, *5*, 212–223.
- (36) Freundlich, H.M.F. Uber die Adsorption in Losungen. *Z. Phys. Chem.* **1906**, *57*, 385–470.
- (37) McKay, G.; Blair, H.S.; Garden, J.R. Adsorption of dyes on chitin. I. Equilibrium studies. *J. Appl. Polym. Sci.* **1982**, *27*, 3043–3057.
- (38) Ashfaq, A.; Clochard, M. –C.; Coqueret, X.; Dispenza, C.; Driscoll, M. S.; Ulański, P.; Al-Sheikhly, M. Polymerization Reactions and Modifications of Polymers by Ionizing Radiation. *Polym.* **2020**, *12*, 2877–2943.
- (39) Davenas, J.; Stevenson, I.; Celette, N.; Cambon, S.; Gardette, J.L.; Rivaton, A.; Vignoud, L. Stability of polymers under ionising radiation: The many faces of radiation interactions with polymers. *Nucl Instrum Methods Phys Res B.* **2002**, *191*, 653–661.
- (40) Ighalo, J. O.; Adeniyi, A. G. A mini-review of the morphological properties of biosorbents derived from plant leaves. *SN Appl. Sci.* **2020**, *2*, 509.
- (41) Manyangadze, M.; Chikuruwo, N. M. H.; Narsaiah, T. B.; Chakra, C. S.; Charis, G.; Danha, G.; Mamvura, T. A. Adsorption of lead ions from wastewater using nano silica spheres synthesized on calcium carbonate templates. *Helvion.* **2020**, *6*, e05309.
- (42) Ma, H.; Liu, B.; Li, B.; Zhang, L.; Li, Y. –G.; Tan, H. –Q.; Zang, H. –Y.; Zhu, G. Cationic Covalent Organic Frameworks: A Simple Platform of Anionic Exchange for Porosity Tuning and Proton Conduction. *J. Am. Chem. Soc.* **2016**, *138* (18), 5897–5903.
- (43) Chen, H.; Tu, H.; Hu, C.; Liu, Y.; Dong, D.; Sun, Y.; Dai, Y.; Wang, S.; Qian, H.; Lin, Z.; Chen, L. Cationic covalent organic framework nanosheets for fast Li-ion conduction. *J. Am. Chem. Soc.* **2018**, *140* (3), 896–899.
- (44) Da, H. –J.; Yang, C. –X.; Yan, X. –P. Cationic Covalent Organic Nanosheets for Rapid and Selective Capture of Perrhenate: An Analogue of Radioactive Pertechnetate from Aqueous Solution. *Environ. Sci. Technol.* **2019**, *53*, 5212–5220.
- (45) Mitra, S.; Kandambeth, S.; Biswal, B. P.; Khayum, M. A.; Choudhury, C. K.; Mehta, M.; Kaur, G.; Banerjee, S.; Prabhune, A.; Verma, S.; Roy, S.; Kharul, U. K.; Banerjee, R. Self-exfoliated guanidinium-based ionic covalent organic nanosheets (iCONs). *J. Am. Chem. Soc.* **2016**, *138* (8), 2823–2828.
- (46) Wilmarth, W. R.; Lumetta, G. J.; Johnson, M. E.; Poirier, M. R.; Thompson, M. C.; Suggs, P. C.; Machara, N. P. Review: waste-pretreatment technologies for remediation of legacy defense nuclear wastes. *Solvent Extr. Ion Exch.* **2011**, *29* (1), 1–48.
- (47) Sun, Q.; Zhu, L.; Aguila, B.; Thallapally, P. K.; Xu, C.; Chen, J.; Wang, S.; Rogers, D.; Ma, S. Optimizing radionuclide sequestration in anion nanotraps with record pertechnetate sorption. *Nat Commun.* **2019**, *10*, 1646–1654.
- (48) Ming, M.; Zhou, H.; Mao, Y. –N.; Li, H. –R.; Chen, Jing. Selective perrhenate/pertechnetate removal by a MOF-based molecular trap. *Dalton Trans.* **2022**, *51*, 4458–4465.
- (49) Zhu, L.; Sheng, D.; Xu, C.; Dai, X.; Silver, M. A.; Li, J.; Li, P.; Wang, Y.; Wang, Y.; Chen, L.; Xiao, C.; Chen, J.; Zhou, R.; Zhang, C.; Farha, O. K.; Chai, Z.; Albrecht-Schmitt, T. E.; Wang, S. Identifying the Recognition Site for Selective Trapping of $^{99}\text{TcO}_4^-$ in a

Hydrolytically Stable and Radiation Resistant Cationic Metal–Organic Framework. *J. Am. Chem. Soc.* **2017**, 139, 14873–14876.